NANO LETTERS

2007
Vol. 7, No. 12
3559−3563

Optical and Electrical Performance of SnO_2 Capped ZnO Nanowire Arrays

Liang Shi,[†] Yeming Xu,[†] Suikong Hark,[†] Yang Liu,[‡] Sheng Wang,[‡] Lian-mao Peng,[‡] Kawai Wong,[†] and Quan Li*,[†]

Department of Physics, The Chinese University of Hong Kong, Shatin, New Territory, Hong Kong, Key Laboratory for the Physics and Chemistry of Nanodevices and Department of Electronics, Peking University, Beijing 100871, China

Received April 4, 2007; Revised Manuscript Received June 7, 2007

ABSTRACT

Two-junction-nanowire arrays (SnO_2 capped ZnO nanowire arrays on Zn substrate) are synthesized using a two-step-solution-reaction. The bare single crystalline ZnO nanowires give reasonably intense band edge luminescence but also strong green emission likely due to surface defects. The SnO_2 capping treatment not only introduces caps on the tip of the ZnO nanowires but also partially passivates the nanowire surfaces, leading to improved near band edge emission and the suppression of the defect luminescence. The nanowire array configuration allows a straight forward electrical measurement on the single nanowire junction (Zn–ZnO–SnO_2). The I–V results indicate that a little barrier exists in between the Zn substrate and the nanowire. The observation of more complicated electrical behaviors of the two-junction system (Zn/ZnO/SnO_2) discloses the nonuniform doping of the SnO_2 cap, which is consistent with the EDX compositional analysis.

Pseudo-one-dimensional nanostructures of ZnO have aroused intense research interests due to their excellent material properties such as the wide band gap and large exciton binding energy that ensures significant excitonic emission at room temperature, leading to a variety of potential applications in optoelectronic nanodevices. Unfortunately, the luminescence properties of these nanomaterials are likely to degrade due to their large surface area, as a result of the unpassivated surface states serving as nonradiative recombination centers, which quench the band edge emission.[1] In this regard, surface passivation can be an effective means to generate desired nanowire surface characteristics and improve the optical properties. Materials of larger band gaps (compared to that of the core material, ZnO in this case) are usually chosen for the surface passivation layer, in order to efficiently confine the electrons and holes within the core material. Successful demonstrations of enhanced photoluminescence from ZnO by surface passivation/modification using physical/chemical approaches[2] have been reported in the recent literature. Nevertheless, how the surface passivation would affect the electrical behavior of the nanowires remains unexplored, although such information is important for the electronic device realization. On the other hand, one shall note that real device applications also require junction formation, which may not exist in most of the as-grown nanostructures. A metal−semiconductor−metal junction nanowire is desired, which not only serves as a basic unit for the optoelectronic nanodevices but also provides an ideal system to study the transport behavior of the nanowires without concerning on the uncertainties of the external contact.

By combining the ideas on surface modification and junction formation, we designed a two-junction nanowire array configuration, using ZnO nanowire arrays grown on the Zn substrate followed by $SnCl_4$ solution treatment, aiming at SnO_2-capped ZnO nanowire array on Zn. SnO_2 is a wide band gap semiconductor with E_g of 3.6 eV and can be easily synthesized via solution reaction of $SnCl_4$ and base.[3] These make it a good candidate for the ZnO nanowire surface passivation due to the simplicity of solution treatment. In addition, doped SnO_2 has been widely used in industries as a transparent electrode, so that capping of ZnO nanowires with doped SnO_2 can lead to the electrode formation directly on the nanowire.

In the present work, we demonstrate that the two-junction nanowire arrays are achieved via a two-step solution reaction, i.e., ZnO nanowire array growth (first step) followed by hydrothermal treatment using $SnCl_4$ solution (second step). Both the ZnO nanowires and the SnO_2 caps are single crystalline with high structural quality. A strong enhancement of the ZnO band edge emission is observed in the SnO_2 capped nanowire, as compared to that from bare ZnO nanowires. Although the Zn substrate−ZnO nanowire junction appears to be ohmic in the electrical measurement, those of the Zn−ZnO−SnO_2 system demonstrate several different

* Corresponding author. E-mail: liquan@phy.cuhk.edu.hk. Tel: (852) 26096323.
[†] The Chinese University of Hong Kong.
[‡] Peking University.

10.1021/nl0707959 CCC: $37.00
Published on Web 11/10/2007

types of I−V characteristics. The formation mechanism of the Zn−ZnO−SnO_2 junction configuration, the capping and passivating effects on the optical properties of ZnO, and electrical properties of the junctions system are discussed.

The fabrication of the SnO_2 capped ZnO nanowire arrays on the Zn substrate is carried in two steps. In the first step, the ZnO nanowire arrays are grown on the Zn substrate via hydrothermal method. In a typical procedure, 10 mL 2M NaOH and 5 mL 30% H_2O_2 are first mixed and stirred before the solution being transferred to a 20 mL stainless steel Teflon-lined autoclave. A piece of 1 × 2 cm zinc foil is then added to the above solution before the autoclave is sealed. The autoclave is then maintained at 190 °C for 8 h before being cooled down to room temperature, when the zinc foil is taken out from the solution and rinsed with distilled water and ethanol, followed by air-drying. In the second step, 0.22 g of $SnCl_4 \cdot 5H_2O$, 5 mL of ethanol, and 5 mL of distilled water are mixed and stirred before the PH value of above solution is adjusted to 12 by adding 2M NaOH (drop by drop). The above solution is then transferred into the 20 mL stainless steel Teflon-lined autoclave, and the product from the first-step-synthesis (a piece of Zn substrate with ZnO nanowires array on it) is added into the autoclave before sealing. The reactor is maintained at 160 °C for 30 h before being cooled down to room temperature. After that, the zinc foil is taken out from the solution and rinsed with distilled water and ethanol and air-dried. Both of the first-step and the final products are examined using the following characterization techniques. The general morphology and crystallinity of the products are examined by scanning electron microscopy (SEM VP1450) and X-ray diffraction (XRD). Transmission electron microscopy (TEM Tecnai 20ST) related techniques are employed to investigate the detailed microstructure of the products. Their luminescence properties are examined using both cathodoluminescence (MonoCL system, Oxford Instrument) at room temperature and temperature-dependent photoluminescence (PL) with samples mounted on a cold finger in a continuous cycle cryostat using the 325 nm line of a HeCd laser. The transport measurements of individual nanowire junctions are carried in a four nanoprobes (MM3A, Kleindiek Company) SEM system (FEI XL 30F).[4]

The first step hydrothermal method using Zn foil as the starting material leads to the growth of ZnO nanowire arrays (Figure 1a), with individual nanowires well-faceted (in the inset of Figure 1a). All of the peaks in the X-ray diffraction of such sample (Figure 1c) can be indexed to hexagonal ZnO (JCPDS No. 36 1451) within the experimental error. In comparison, although the $SnCl_4$ solution treated nanowire sample maintains the nanowire array morphology, octahedral shaped tips (in the inset of Figure 1b) are found on the ZnO nanowires (Figure 1b). X-ray diffraction taken from such sample (Figure 1c) suggests the existence of another material than ZnO, i.e., SnO_2 with orthorhombic structure (JCPDS No78 1063). The SnO_2-capped ZnO nanowire morphology (in contrast with SnO_2-tipped ZnO nanowire) is first suggested by the low magnification TEM image of single nanowire (Figure 2a). One would notice the wire-like contrast

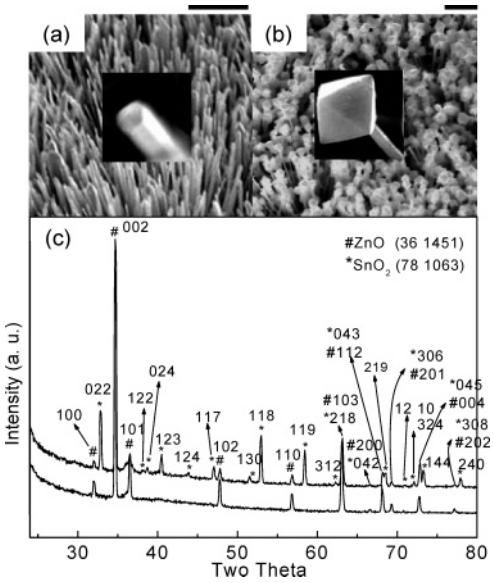

Figure 1. SEM images of (a) aligned ZnO nanowires grown on Zn substrate and (b) SnO_2 capped ZnO arrays, enlarged single wires with and without cap are shown in the center inset of (a) and (b); The scar bars in the figure are 1 μm in length. (c) X-ray diffraction taken from bare and SnO_2 capped ZnO nanowires.

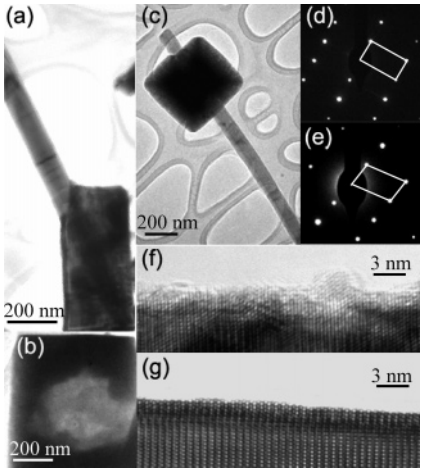

Figure 2. Low magnification TEM images showing (a) single ZnO nanowire capped by SnO_2 with the ZnO tip buried inside the SnO_2 cap; (b) a falloff SnO_2 cap; and (c) SnO_2 wrapping the ZnO nanowire at lower positions with the nanowire tip exposed. (d and e) The TEDs taken from the wire and the cap part can be indexed to single crystalline ZnO (hexagonal), and SnO_2 (orthohombic), respectively; (f) and (g), The high-resolution TEM images showing the surface of the ZnO nanowire after, and before the $SnCl_4$ solution treatment, respectively.

in the center part of the rectangle-shaped tip, indicating that the SnO_2 wraps the ZnO nanowire, instead of forming a sharp SnO_2 (tip)−ZnO (wire) transition along the nanowire growth direction. Further experimental evidence comes from the TEM observation of some of the falloff caps, in which a center hole is visible (Figure 2b). In fact, a small amount of the SnO_2 particles are wrapping the ZnO nanowires at slightly lower position below the nanowire tip, leaving the tip being exposed (Figure 2c). Corresponding SEM images of such nanowires can be found in the Supporting Information. Both of the ZnO nanowire and the SnO_2 cap are single crystalline,

as suggested by the electron diffraction patterns taken from the wire (Figure 2d) and cap (Figure 2e), respectively. The diffraction patterns shown in Figure 2, panels d and e, can be indexed to hexagonal ZnO (100) zone axis and orthorhombic SnO_2 ($\bar{4}11$) zone axis, respectively, being consistent with the XRD results. Defocused diffraction studies on several tens of ZnO nanowires disclose that all of ZnO wires grow along their [001] crystalline direction (*c* axis). Although EDX analysis of the ZnO nanowire portion reveals a composition of Zn and O only, those taken from the SnO_2 cap portion suggests the existence of mainly Sn and O, together with a small percentage of Zn in the range of 1−10%. The surface of the SnO_2 capped ZnO nanowire appears to be rough (Figure 2f), as compared to that of the as-grown ZnO nanowire (without the second step $SnCl_4$ solution treatment) shown in Figure 2g. By comparing the HREM data, although the surface of the ZnO nanowire appears to be modified after the $SnCl_4$ solution treatment, no obvious surface layer can be identified in imaging. Elemental mapping has also been preformed on the samples in order to find out the spatial distribution of the compositional elements (provided in the Supporting Information). However, it is difficult to determine the surface composition of the ZnO nanowire (other than Zn and O), as limited by the sensitivity of such technique.

We first discuss the growth mechanism of the ZnO nanowire arrays on the Zn foil. In the first step hydrothermal process, H_2O_2 serves as a strong oxidant for the Zn foil in the alkaline solution of NaOH. The Zn foil would be readily oxidized starting with a large amount of ZnO nanoclusters on the foil surface. These nanoclusters become the nuclei for further ZnO crystal growth as the oxidation proceeds. With ZnO's natural tendency of anisotropic growth along the crystalline *c* axis,[5] the produced strong oxidizing environment serves as a kinetic driving force and promotes the anisotropic development and thus the growth of elongated nanocrystals.[6] As a result, ZnO nanowire arrays on the Zn substrate are formed with all of the nanowires growing along the crystalline *c* axis.

The chemical reaction $Sn^{4+} + 4OH^- = SnO_2 + 2H_2O$, which is well-documented in the literature,[7] occurs in the second step of synthesis. The orthorhombic phase of SnO_2, although metastable at ambient conditions, is quite common in the products of the hydrothermal reactions.[8] The ZnO nanowire arrays on the Zn substrate serve as a "template" for the SnO_2 cap growth; although fully soaked in the Sn^{4+} solution, the complete contact in between the nanowire array and the solution should be limited to the nanowire tip region, due to the nonwettable nature of water on such nanostructures.[9] The ZnO tip region therefore serves as the preferential nucleation site for the SnO_2, resulting in the cap growth. In addition, the basicity environment in the solution also leads to formation of Zn containing ions owing to the reaction in between Zn and the base. These Zn containing ions contribute to the doping of the SnO_2 particles during their growth. Control experiment without adding the ZnO nanowire arrays in the reactor only leads to formation of ill-shaped but chemically pure SnO_2 particles. Although most parts of the

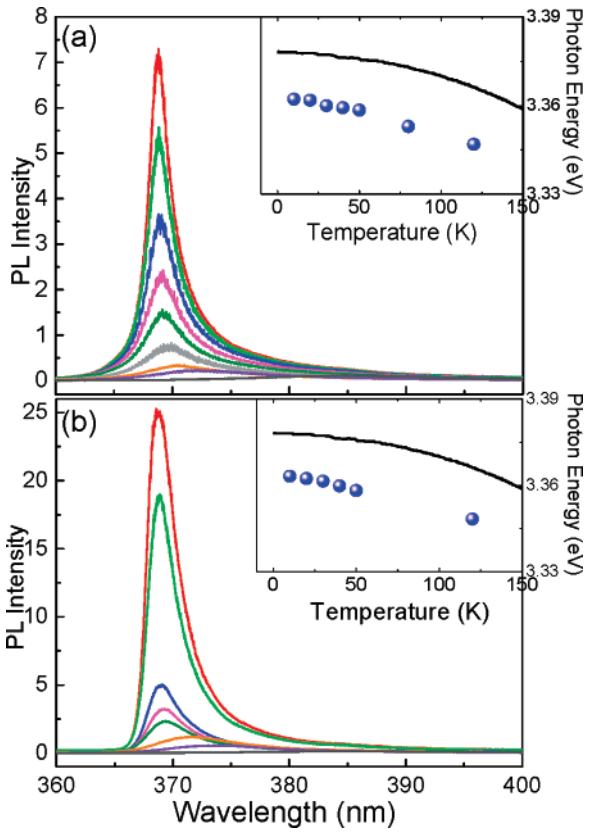

Figure 3. Temperature-dependent PL spectra taken from (a) the bare ZnO and (b) the capped ZnO nanowires from room temperature to 10 K.

ZnO nanowire surfaces would not be in direct contact with the solution, ion/molecule diffusion along the nanowire surface could occur. A similar reaction that results in the formation of SnO_2 as in the solution would take place but at a much smaller scale, due to the limited availability of Sn^{2+} and OH^- on the ZnO nanowire surface away from the tip region. This leads to some surface passivation of the nanowires but not thick surface layer growth. One should note that the surface passivation at the monolayer scale may not be easily observed by microstructural characterizations using conventional TEM but can lead to significantly different optical behavior of the ZnO nanowires, as will be discussed in later sections.

A distinct intensity difference of the near band edge emission (NBE) from the bare and the SnO_2 capped ZnO nanowires is observed in the photoluminescence (PL) study of the two (Figure 3), in which the NBE intensity from the SnO_2 capped ZnO nanowire is more than three times stronger than that of ZnO nanowires without the SnO_2 cap. The temperature-dependent PL study shows that both samples give the band edge emission at 386 nm at room temperature, which blue shifts as the temperature goes down and eventually reaches 369 nm at 10 K. The temperature dependences of the photon energies of both samples are plotted in the insets of Figure 3, panels a and b, in which the solid line is the band gap data from reference.[10] It is seen that these peaks essentially track the band gap.

Consistent results are obtained from the room-temperature cathodoluminescence (CL) measurements of the nanowire

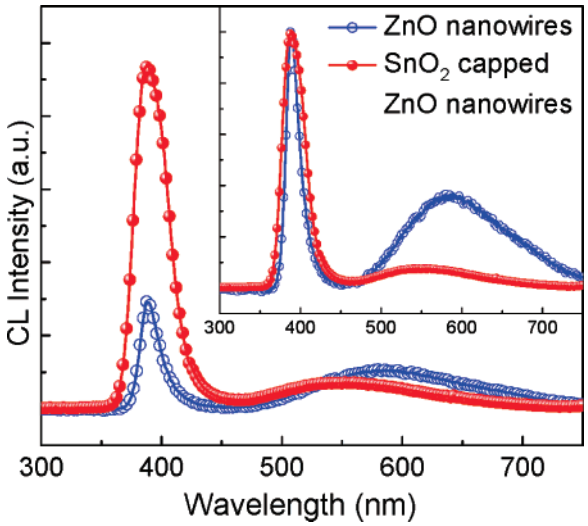

Figure 4. CL spectra taken from the bare ZnO and capped ZnO nanowires showing their differences in both the near band edge emission and the deep level emissions under the same excitation condition. The upper right inset shows the NBE/DLE ratio comparison of the two spectra with their NBE intensity normalized.

samples before and the after the solution treatment. Both samples give a NBE at ~386 nm with a stronger intensity observed in the SnO_2 capped ZnO nanowires. In addition, a broad deep level emission (DLE) is observed in the bare ZnO nanowire sample. The peak center and the intensity of such DLE are found to be different with and without the cap. The comparison of their NBE/DLE ratios can be found in the inset of Figure 4, with their NBE intensity normalized.

The near band edge emission of the bare ZnO nanowire is generally interpreted as originating from excitonic recombinations. At room temperature, the possible existence of different types of donors and acceptors in the ZnO nanowire (impurities introduced during the growth process) leads to multiple excitons of slightly different binding energies, all of which contribute to the near band edge emission, resulting in a broad peak. As the temperature goes down, only one major peak feature become intense, while its broadened width suggests the existence of other unresolved peaks associated with the splitting of the valence band structure. Judging from the dominant peak position and its temperature dependence in the PL measurement, such a peak may be assigned to excitons bound to neutral donors or acceptors. The observation of the excitonic emission and the similarity of peak characteristics in the PL measurements in both samples (bare and SnO_2 capped ZnO nanowires) indicate the good electronic structure quality of the ZnO nanowire interior, which has not been degraded after the SnO_2 capping.

The green emission is commonly ascribed to be defect related, particularly those native defects such as O vacancies and Zn interstitials.[11] In the case of nanowires, numerous studies in the literature suggest that such defect emission is surface-dependent, due to the surface dominance of the native defects.[1] It has been found that the defect luminescence grows at the expense of the near band edge emission in small diametered nanowires and is expected to quench the NBE in the extreme cases.[12] In this regard, one shall expect that

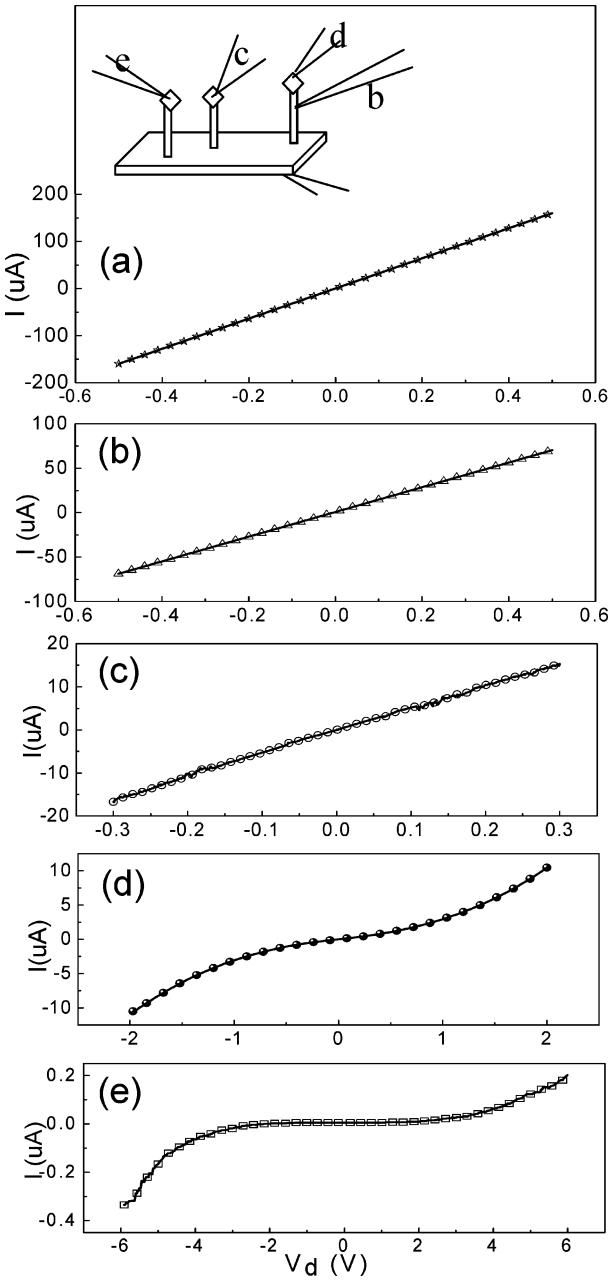

Figure 5. Electrical measurements of (a) ZnO nanowire by locating both of the probes on two different locations on the nanowires; (b) the Zn−ZnO junction, showing linear I−V characteristic, and Zn−ZnO−SnO_2 junctions, showing both linear (c) and nonlinear (d and e) features in the I−V curves. The schematic of the measurements (b−e) can be found in the inset of (a).

surface passivation of the nanowires would improve their luminescence properties, which has been observed in the present work.

In other words, the hydrothermal treatment indeed has an important impact on the optical properties of the ZnO nanowires. The improved NBE intensity and the suppressed defect emission can be understood from the following aspects. First, the larger band gap of the SnO_2 compared to that of ZnO more efficiently confines the electrons/holes in the ZnO nanowires, the recombination of which pairs gives the near band edge emission. In addition, the surface dangling bonds and/or surface defect density of states can be reduced

via the surface passivation. All of these contribute to the increased NBE and the suppressed DLE. In fact, the shift of the DLE peak center (observed in CL) is a piece of direct evidence of the modified nanowire surface properties, given that such green luminescence mainly originates from the surface defects of the ZnO nanowires.[12]

To investigate the transport properties of the nanowire junction system, we employed a four probe SEM system to carry the electrical measurements on a single nanowire junction. A schematic of such a measurement can be found in the inset of Figure 5. We first measure the electrical behavior of a single ZnO nanowire by locating two probes on the two side of the nanowire (without touch either the Zn substrate or the SnO_2 tip). A linear I−V characteristic is observed (Figure 5a), and the data is reproducible for all of the ZnO nanowires measured. The single junction in between the ZnO nanowire and the Zn substrate is measured by two probes, when the linear I−V characteristic is always found (Figure 5b), based on a number of individual nanowires measured. The Ohmic contact and the low resistivity of such a measurement disclose that the ZnO nanowires are highly doped, with the dopant likely being introduced during the growth process (first step solution growth). Different I−V behaviors are observed when the two-junction system (Zn−ZnO−SnO_2) is measured. Although some of the two-junction nanowires demonstrate linear I−V behavior (but with different resistivities in different nanowire measured; Figure 5c), others show nonlinear behavior (Figure 5d,e), indicating the existence of barriers. Such a drastic difference in the electrical behavior may result from the different doping level of the SnO_2 tips, which has been suggested by the EDX analysis of several tens of such tips, giving a fairly large range of Zn concentration. A detailed understanding of the electrical behavior of these two-junction nanowires requires further study and is currently under investigation.

In conclusion, SnO_2 capped ZnO nanowire arrays on Zn substrate have been realized via a two-step hydrothermal growth. The single crystalline ZnO nanowires give reasonably intense band edge luminescence but also strong green emission likely due to surface defects. Experimental evidence demonstrates that the hydrothermal treatment using $SnCl_4$ + H_2O_2 not only induces the SnO_2 cap growth in the tip region of the nanowires but also partially passivates the surface of the nanowires, both of which contribute to the improved near band edge emission and the suppression of the defect luminescence. The nanowire array configuration also allows a straight forward electrical measurement on the single nanowire junction (Zn−ZnO−SnO_2). The I−V results indicate that the ZnO nanowires are highly doped, and little barrier exists in between the Zn substrate and the nanowire; that is, the surface passivation does not introduce any barrier in the electrical measurement. The observation of more complicated electrical behaviors of the two-junction system (Zn/ZnO/SnO_2) discloses the nonuniform doping of the SnO_2 cap, which is consistent with the EDX compositional analysis. Nevertheless, the observed linear I−V characteristic in some of the two-junction nanowires indeed suggests the possibility of using highly doped SnO_2 as the electrode grown on the ZnO nanowire and thus constructing ideal device configuration: ZnO nanowire arrays naturally grown with two electrodes at both ends with little barrier at the junction interfaces.

Acknowledgment. This work is supported by grants from the Research Grant Council of the HKSAR under Project No. 413706 and National Science foundation of China under Grant No. 10434010.

Supporting Information Available: SEM images of nanowires and elemental mapping. This material is available free of charge via the Internet at http://pubs.acs.org.

References

(1) Yao, B. D.; Chan, Y. F.; Wang, N. *Appl. Phys. Lett.* **2002**, *81*, 757−759. Chiou, J. W.; Krishna Kumar, K. P.; Jan, J. C.; Tsai, H. M.; Bao, C. W.; Pong, W. F.; Chien, F. Z.; Tsai, M. H.; Hong, I. H.; Klauser, R.; Lee, J. F.; Wu, J. J.; Liu, S. C. *Appl. Phys. Lett.* **2004**, *85*, 3220−3222.

(2) Lin, J. M.; Cheng, C. L.; Lin, H. Y.; Chen, Y. F. *Opt. Lett.* **2006**, *31*, 3173. Lin, C. C.; Chen, H. P.; Liao, H. C.; Chen, S. Y. *Appl. Phys. Lett.* **2005**, *86*, 18. Li, J. H.; Zhao, D. X.; Meng, X. Q.; Zhang, Z. Z.; Zhang, J. Y.; Shen, D. Z.; Lu, Y. M.; Fan, X. W. *J. Phys. Chem. B* **2006**, *110*, 14685.

(3) Zhang, D. F.; Sun, L. D.; Yin, J. L.; Yan, C. H. *Adv. Mater.* **2003**, *15* (12), 1022. Guo, C. X.; Cao, M. H.; Hu, C. W. *Inorg. Chem. Commun.* **2004**, *7* (7), 929−931.

(4) Peng, L.-M.; Chen, Q.; Liang, X. L.; Gao, S.; Wang, J. Y.; Kleindiek, S.; Tai, S. W. *Micron* **2004**, *35*, 495−502.

(5) Vayssieres, L.; Keis, K.; Lindquist, S.; Hagfeildt, A. *J. Phys. Chem. B* **2001**, *105*, 3350; Vayssieres, L.; Yi, G.; Kim, M.; Lindquist, S. *Chem. Mater.* **2001**, *13*, 4395.

(6) Tang, Q.; Zhou, W.; Shen, J.; Zhang, W.; Kong, L.; Qian, Y. *Chem. Commun.* **2004**, *21* (6), 712−713. Peng, X. *Adv. Mater.* **2003**, *15*, 459.

(7) See ref 3.

(8) *J. Appl. Phys.* **2004**, *96* (11), 6195−6200.

(9) Feng, X. J.; Jiang, L. *Adv. Mater.* **2006**, *18*, 3063.

(10) Teke, A.; Ozgur, U.; Dogan, S.; Gu, X.; Morkoc, H.; Nemeth, B.; Nause, J.; Everitt, H. O. *Phys. Rev. B* **2004**, *70*, 195207.

(11) Vanheusden, K.; Seager, C. H.; Warren, W. L.; Tallant, D. R.; Voigt, J. A. *Appl. Phys. Lett.* **1996**, *68*, 403.

(12) Shalish, I.; Temkin, H.; Narayanamurti, V. *Phys. Rev. B* **2004**, *69*, 245401.

NL0707959